UNISDR
The United Nations Office for Disaster Risk Reduction

GAR
Global Assessment Report on Disaster Risk Reduction
2013

Background Paper prepared for the Global Assessment Report on Disaster Risk Reduction 2013

Localized Flooding Hazard Computation

Roberto Rudari
CIMA Research Foundation International

RESEARCH FOUNDATION
cima
OBSERVE TO PREDICT, PREDICT TO PREVENT.

Geneva, Switzerland, 2013

FINAL REPORT

Objective 2: Localized Flooding Hazard computation
Expected outcome: Compelling examples on small islands for localized Flooding
Indicators of achievement: Final Report and Localized Flooding maps

1.1 Background

In densely urbanized areas with local flat spots, intense rainfall events can trigger local flooding due to prolonged and extended ponding. Two main causes identify areas prone to ponding: morphology and the limited drainage capacity of the natural and manmade network. These events might not be as devastating as river flooding, but their frequency is very high and therefore their impact on society.

The knowledge of areas potentially prone to flooding can be extremely useful for planning and civil protection actions, and in certain cases (i.e., small islands) is an important part of the global risk assessment of the area.

In literature we find a large number of inundation models, but few of them can be applied at regional or global scale, and furthermore they often neglect local ponding effects.

CIMA Research Foundation developed a ponding model based on concept taken from Self Organized Criticality (SOC). Specifically, the model was inspired by the sandpile model (per Bak, 1996). The sandpile model has been modified so that it can be applied to a multisource phenomenon like local flooding.

The model assumes that the interactions among local and far morphological features, slope, soil use and type allow the identification of ponding prone areas.

In the particular context of GAR such model can be of dramatic help in identifying risk in Small Islands Developing States (SIDS), which often lack of a well organized river network and are exposed to torrential rains, so that local flooding is on e of the major threats they experience. SIDS have pronounced topography with sudden changes in slope, this concentrates in ponding areas large amounts of rainwater causing huge problems to facilities and lifelines considering also the quality of infrastructure and the large number of unpaved roads.

The areas of application of the model have been therefore the Caribbean Islands in the present Work. The model outputs a probabilistic information (ponding Likelihood) starting from DTMs and digital Land Use maps.

1.2 Proposed Methodology

The model develops on the idea of the “sandpile” model, which is a consolidated models in the SOC literature (Bak, 1996). These models have the interesting feature of reproducing properly patterns deriving from complex interactions in nature by means of simple rules and few control parameters. Furthermore, such parameters do not need extensive calibration because they aim at represent processes in terms of their relative importance with respect to the other competing processes. Specifically, the structure of the model imposes to get right the order of magnitude of the two competing processes: the local drainage/storage capacity and the flooding water concentration and expansion. This should ensure a proper pattern recognition. The fact of utilizing a SOC to model pluvial flooding is crucial as few times there are input-output data that allow modelers to perform a proper cal/val experiment.

The sandpile models is a “multisource” model of spatial diffusion, and as such is it can be used to represent the local flooding phenomenon. The model however have been deeply modified to fully represent the local flooding mechanism. Specifically it was necessary to represent in the model the natural drainage network as well as the sub-surface hydraulic connection.

1.2.1 Input data

The ponding model uses easy-to-find data world wide such as:
- digital elevation maps (DEMs), to define altitudes and the drainage network directions
- detailed land use maps and possible soil type maps to derive soil hydraulic characteristics
- precipitation maps (that can be synthetically determined from local climatology)

the model parameter are the local drainage capacity and the flooding velocity of contiguous cells. This last parameter represents the velocity at which, once the drainage capacity is overcome, the cells contiguous to the source cell are flooded. These parameters maintain a reasonable physical meaning can be calibrated in a very simple way as that should represent not exact values of the physical quantity, but the order of magnitude of the processes they represent in the model. They, in fact, represent two competitive processes that influences the extension and the duration of the flooding.

With regards to the Caribbean SIDS implementation the data used have been the following:

- DEM: The Advanced Spaceborne Thermal Emission and Reflection Radiometer (ASTER) Global Digital Elevation Model (GDEM) version 2[1] developed jointly by the U.S. National Aeronautics and Space Administration (NASA) and Japan’s Ministry of Economy, Trade, and Industry (METI).
- LandUse: various sources including local land use maps provided by the Countries (e.g. Barbados), CORINE maps of the French DOMs available from the Ministère de l’Écologie, du Développement Durable et de l'Énergie, *Commissariat général au Développement durable*[2]; Data from International Institute of Tropical Forestry available form the Forest Service of the USDA web site[3] based on Landsat imagery (Helmer et al., 2008; 2012, Kennaway et al., 2007; 2009)

1.2.2 Model structure

Each pixel in which the domain is subdivided can be seen as a reservoir characterized by:

- Soil retention capacity, and for urban soil a drainage capacity offered by the sewing system, which regulate saturation from below, such retention capacity is based on the CN value (SCS – CN method) that is eventually derived from Land Use maps.
- A threshold on the rainfall intensity that mimics the runoff production for rainfall excess. Such threshold is based on the CN value (SCS – CN method) that is eventually derived from Land Use maps and on the local slope value as computed from the DEM information.

[1] https://lpdaac.usgs.gov/products/aster_products_table/astgtm
[2] http://www.statistiques.developpement-durable.gouv.fr/donnees-ligne/t/telechargement-donnees-sig-corine-land-cover-dom.html

[3] http://fsgeodata.fs.fed.us/rastergateway/caribbean/

The water transfer on the surface drainage network is a function of slope while flooding is based on the comparison between the hydraulic depths of the contiguous cells with flooding intensity proportional to the water depth gradients (representing the free water surface slope.)

Figure 1 shows the schematics of the water transfer mechanism between cells in the algorithm.

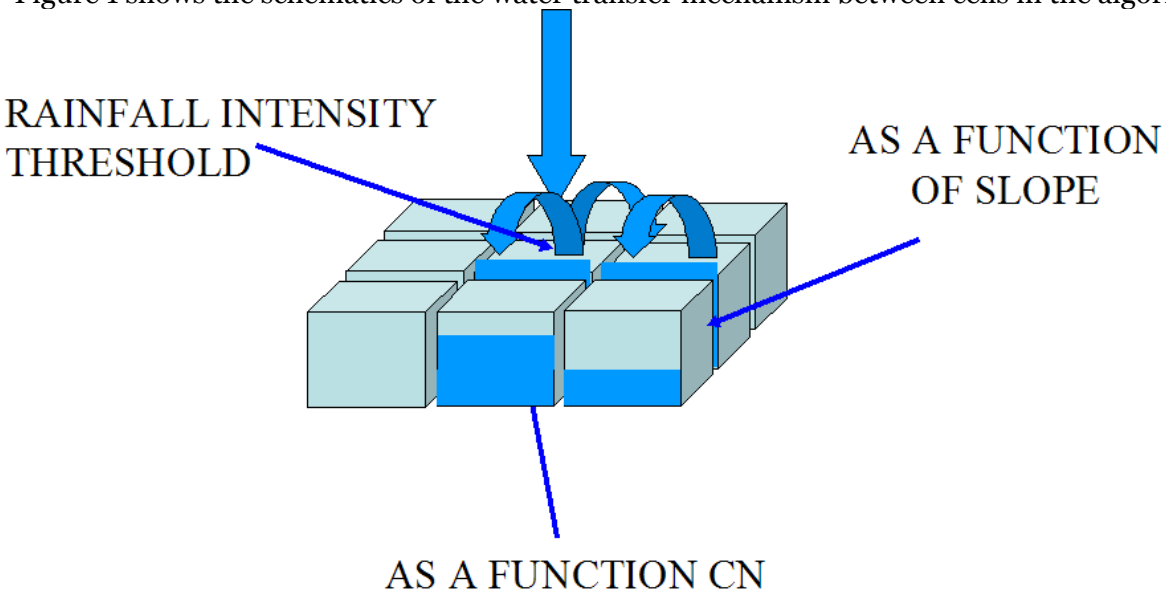

Figure 1 water transfer scheme in the algorithm. Saturation from below is a function of the infiltration capacity described by the Curve Number (SCS Method).

1.3 Static Ponding hazard maps for Caribbean Islands

The local flooding model has been applied in some of the Caribbean SIDS. The choice of the SIDS mainly driven by the availability of reliable Land Use information at the neded resolution (i.e. 30 metres). The following list summarizes the Caribbean Islands where the model was applied to obtain local flooding Hazard maps:

1. Virgin Island
2. Barbados
3. British Virgin Islands
4. St Kitts and Nevis
5. Grenada
6. Trinidad
7. Tobago
8. Puertorico
9. Isla de Mona
10. Guadeloupe
11. Martinique
12. Marie Galante
13. Monserrat
14. Anguilla

The results are produced at 30 m resolution that is the resolution of the DEM used.

The results are released in terms of water depths for different return periods (T=2, 5, 10, 25, 50, 200, 500, 1000 years) For each return period 100 scenarios are built so that it is possible to

derive not only the maximum water depths maps but also a standard deviation map that characterizes the whole modelling chain uncertainty and allows for ensemble scenarios production.

The procedure model to determine the ponding hazard maps is depicted in Figure 3.

The procedure starts from rainfall analyzing the rainfall climatology on the area. Usually this part would be based on traditional gauge observations showing adequate time series length. The Caribbean areas suffers from a lack of such information. Just few observation points where available for the computation of Intensity Duration Curves (IDFs), specifically Bahamas, Cayman Islands, Montserrat, St. Vincent, Trinidad and Tobago.

IDFs where computed for the sites. Additional the TRMM data have been processed to produce areal average rainfall information in the Caribbean Islands from 1998 to Present. Such a time length allowed us to computed TRMM based IDFs for the Caribbean Region at large. However it is well known that TRMM data tend to underestimate rainfall and therefore IDF results are expected to be biased. The Bias between TRMM derived IDFs and the ones computed on the basis of the ground observations have been computed. Such a bias was reasonably constant geographically. The bias is a weak function of Return Period (i.e. rainfall intensity) while the dependency was found with rainfall duration. The dependence on duration is fairly linear, identifying a constant additive bias. Based on the about findings we defined a liner bias correction function for the Region.

In this way it was possible to derive bias corrected IDFs for the whole Caribbean SIDS (Figure 2).

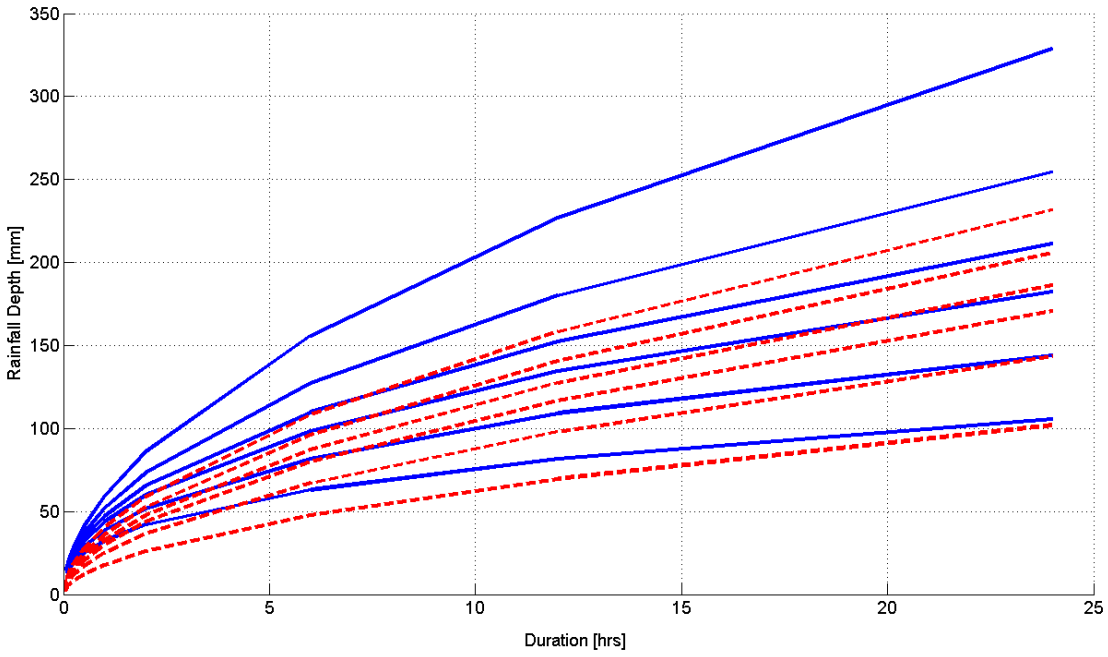

Figure 2 Example of IDF curve for the Virgin Island for T=2, 5, 10, 25, 50, 200, 500, 1000 years. The red dashed curves are the TRMM derived IDFs, while the blue continuous curves are the bias corrected IDFs.

It is possible to compute rainfall values at Island scale. Such uniform values are then downscaled at the DEM resolution and at sub hour scale using a stochastic downscaling procedure called RainFARM (Rebora et al 2006). Once such maps are available at spatial and temporal scales which are appropriate for the model, then the model is run for an ensemble of

equiprobable events of pre determined temporal length (12 hours in this case). The results are then post processed to produce a Maximum Water Depth map each return period and a standard deviation map, again for each return period.

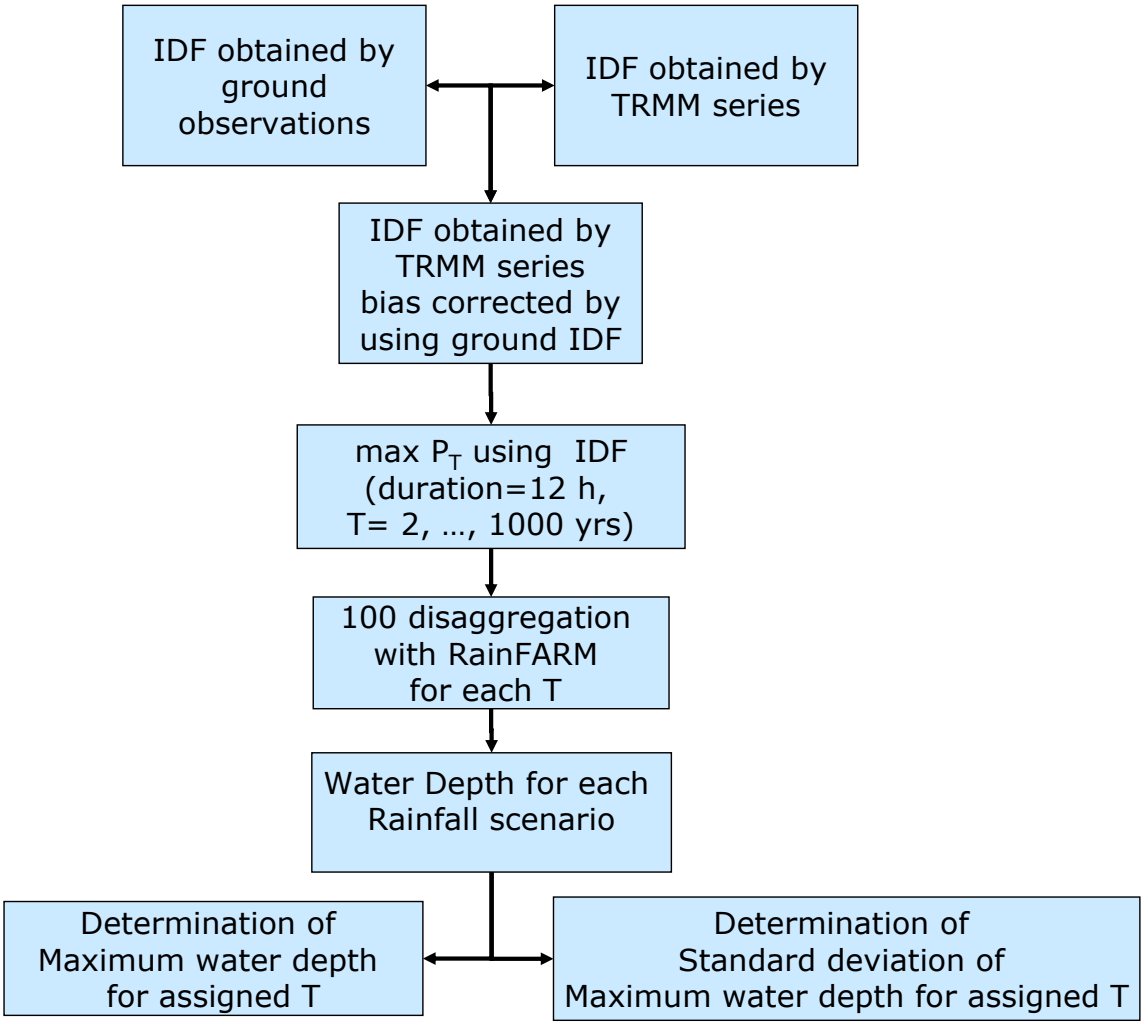

Figure 3 Scheme for the model run: computation of ponding hazard maps

In the following an example of ponding hazard map is presented with reference to the Island of Barbados. Figure 4 shows a corography of the island of Barbados which is chosen here to present the ponding model results.

Figure 4 Corography of the Barbados island.

The island of Barbados has a detailed High quality DTM with a 10 m resolution (Figure 5). The DEM has been processed to extract drainage directions as well as Drained area map and slope maps (Figure 5), which are necessary for the model run. The island has a marked orography and some valleys characterized by galleys are visible. The urbanized area concentrates mostly in the south western part of the Island and it is where we expect ponding hazard to be mostly present.

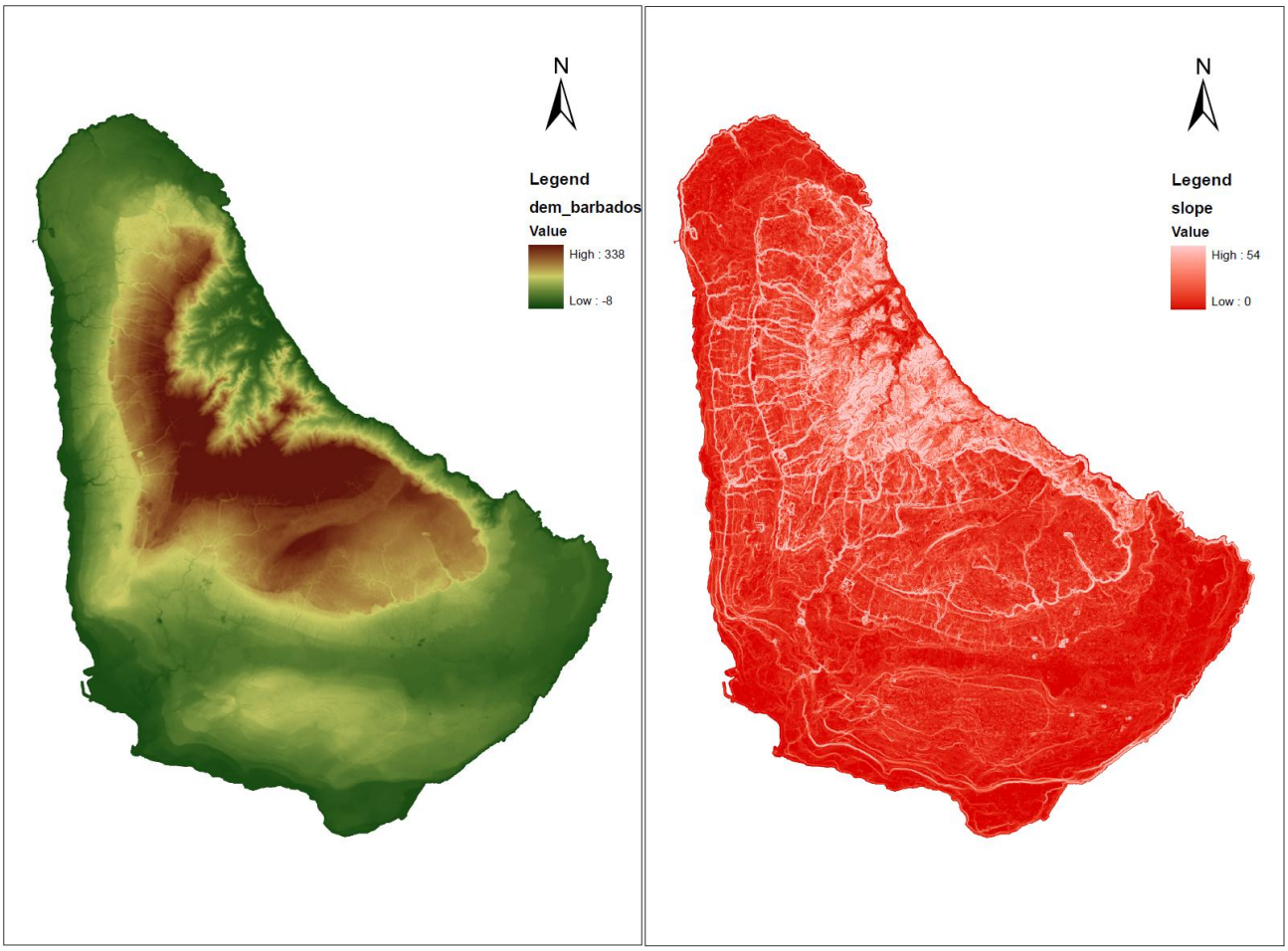

Figure 5 DTM of the Island on Barbados (resolution of the Grid 10 metres), Slope derived map of the Island of Barbados.

Figure 6 shows the soil use map of the island of Barbados which is elaborated to be transformed into a Curve Number map, that describes the soil hydraulic properties to be used by the model for the infiltration characterization (CN = 100 no infiltration potential, Low CN = high infiltration potential). The conversion table is reported in Table 1 for the values of the soil use map. In addition to the soil use fields additional information about roads and buildings were available in the case of Barbados and have been used to determine the final CN map. Where additional ancillary information were available (e.g. OpenStreetMap polygons) such information have been used to complement the final CN maps. In principle land use alone is not enough to properly assign a CN value. Soil permeability would be needed as well. however, soil type information was hardly available on the Caribbean SIDS. This is less important in urbanized areas, but has impact in more natural environments. It has to be consider that a strong correlation, especially in less urbanized area, exists between vegetation cover and soil type, so that land use can be considered a good aggregated proxy of the combination of land cover and soil type.

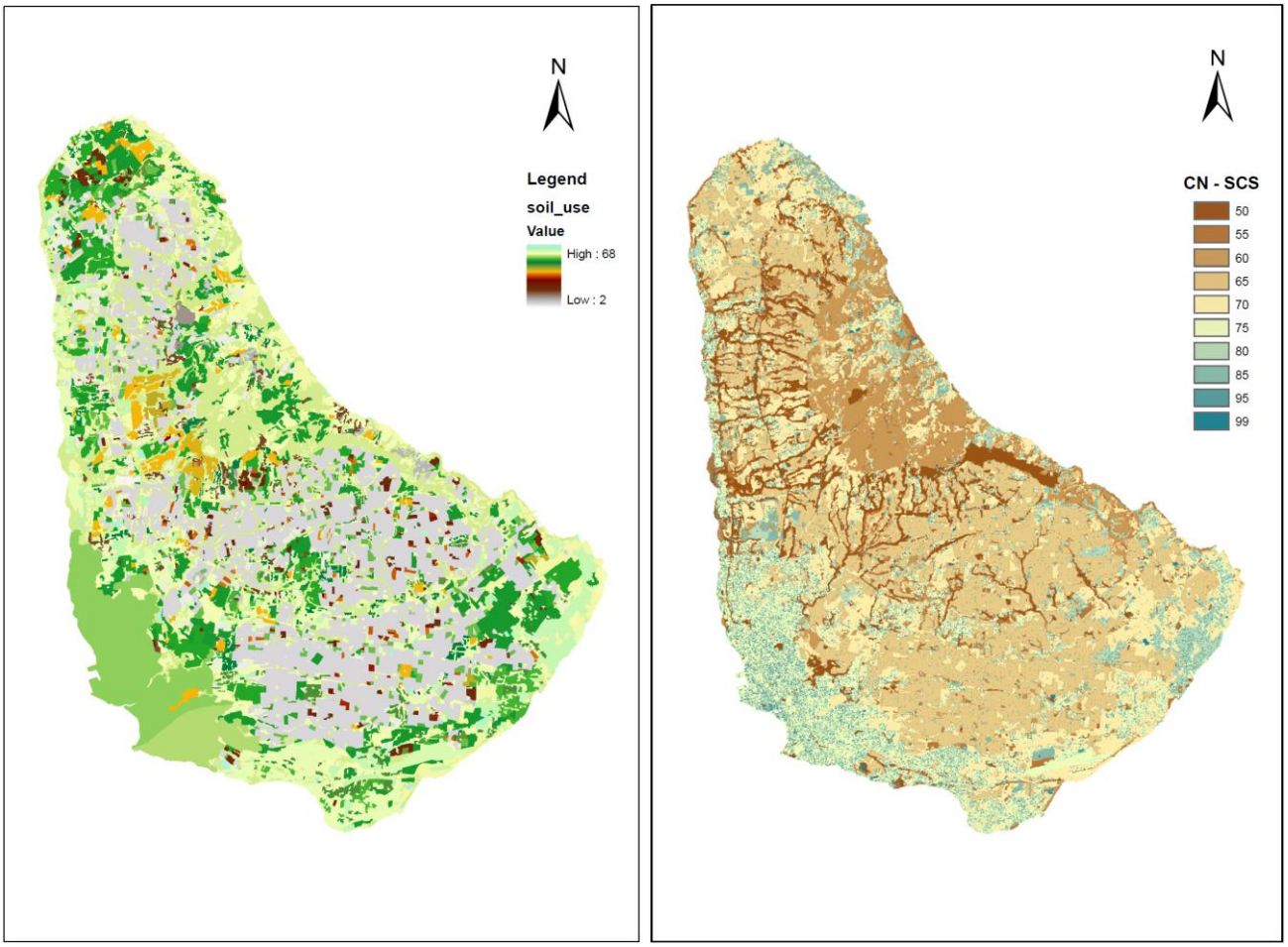

Figure 6 Soil use Map (legend using numeric codes reported in Table 1 and their transformation into Curve Numbers map.

High infiltration potential are assigned to plantations and forests while a low infiltration potential is concentrated in the urban areas.
Since the land cover maps originated from different sources a simplified table was also adopted for Land cover – CN conversion (Table 2).

CLASS	DESCRIPTION	GROUP	TYPE	SUB-TYPE	id	COD CORINE	CN
1					1	111	90
1					2	111	85
1	Sugar cane	Sugar Cane	Agriculture	Sugar Cane	3	211	60
623	Cane fields/gardens	Sugar Cane	Agriculture	Sugar Cane	4	211	60
4	Mixed cane fields/bananas	Sugar Cane	Agriculture	Sugar Cane	5	211	60
708	Plantation crop	Sugar Cane	Agriculture	Sugar Cane	6	211	60
88	Orchards	Tree Crops	Agriculture	Predominantly fruit trees	7	222	60
35	Mixed orchard	Tree Crops	Agriculture	Predominantly fruit trees	8	222	60
97	Pure stands	Tree Crops	Agriculture	Predominantly fruit trees	9	222	60
9	Small stands mixed with food cro	Mixed	Agriculture	Vegetables	10	244	70
11	Cherry	Tree Crops	Agriculture	Cherry	11	222	60
9	Citrus	Tree Crops	Agriculture	Citrus	12	222	60
27	Coconuts	Tree Crops	Agriculture	Coconuts	13	222	60
4	Guava	Tree Crops	Agriculture	Guava	14	222	60
6	Mango	Tree Crops	Agriculture	Mango	15	222	60
3	Papaya	Tree Crops	Agriculture	Papaya	16	222	60
2	Pineapple	Tree Crops	Agriculture	Pineapple	17	222	60
15	Mixed quava/mango/citrus	Tree Crops	Agriculture	Predominantly fruit trees	18	222	60
261	Settlement trees	Tree Crops	Agriculture	Settlement trees	19	222	60
12	Food crops	Vegetables	Agriculture	Food crops	20	211	60
58	Mixed vegetables/root crops	Vegetables	Agriculture	Vegetables	21	211	60
22	Vegetables	Vegetables	Agriculture	Vegetables	22	211	60
207	Mixed vegetables	Vegetables	Agriculture	Vegetables	23	211	60
10	Beans	Vegetables	Agriculture	Beans	24	211	60
7	Cabbage	Vegetables	Agriculture	Cabbage	25	211	60
63	Carrots	Vegetables	Agriculture	Carrots	26	211	60
52	Maize	Vegetables	Agriculture	Maize	27	211	60
82	Onions	Vegetables	Agriculture	Onions	28	211	60
9	Peanuts	Vegetables	Agriculture	Peanuts	29	211	60
1	Pumpkin	Vegetables	Agriculture	Pumpkin	30	211	60
4	Sorghum	Vegetables	Agriculture	Sorghum	31	211	60
15	Root crops	Vegetables	Agriculture	Root crops	32	211	60
83	Mixed root crops	Vegetables	Agriculture	Mixed root crops	33	211	60
11	Casssava	Vegetables	Agriculture	Casssava	34	211	60
18	Eddoes	Vegetables	Agriculture	Eddoes	35	211	60
115	Sweet potatoes	Vegetables	Agriculture	Sweet potatoes	36	211	60
133	Yams	Vegetables	Agriculture	Yams	37	211	60
36	Ginger lilies + Heliconia + Anthur	Ornamental	Agriculture	Ornamental	38	211	60
1	Nursery	Ornamental	Agriculture	Ornamental	39	211	60
140	Improved pasture / livestock unit	Animal Husbandry	Agriculture	Animal Husbandry	40	321	75
9	Beef cattle	Animal Husbandry	Agriculture	Animal Husbandry	41	321	75
34	Dairy cattle	Animal Husbandry	Agriculture	Animal Husbandry	42	321	75
2	Horses	Animal Husbandry	Agriculture	Animal Husbandry	43	321	75
1	Poultry	Animal Husbandry	Agriculture	Animal Husbandry	44	321	75
3	Sheep	Animal Husbandry	Agriculture	Animal Husbandry	45	321	75
65	Cotton	Cotton	Agriculture	Cotton	46	212	60
823	Predominantly food crops	Mixed	Agriculture	Vegetables	47	211	60
173	Predominantly fruit trees	Tree Crops	Agriculture	Predominantly fruit trees	48	211	60
467	Mixed cane / fruit trees / food cro	Mixed	Agriculture	Vegetables	49	244	70
76	Un[der]-productive [i.e. idle] agric	Pastureland	Agriculture	Pastureland	50	321	75
561	Abandoned agricultural land	Pastureland	Agriculture	Pastureland	51	321	75
327	Sugar Cane	Sugar Cane	Agriculture	Sugar Cane	52	211	60
317	Abandoned gardens	Pastureland	Agriculture	Pastureland	53	321	75
625	Fallow [open] land; no crop curre	Pastureland	Natural	Natural	54	321	75
2					55	111	95
1					56	111	95
1915	Trees and tree-shrub	Pastureland	Natural	Natural	57	321	75
804	Grassland [rough unimproved pa	Pastureland	Natural	Natural	58	321	75
1189	Grassland-shrub	Pastureland	Natural	Natural	59	321	75
2689					60	111	90
89					61	111	90
224					62	111	90
2					63	111	90
30					64	111	90
6					65	111	90
77					66	111	90
95	Open water	Natural	Natural	Natural	67	512	99
2	Swamp	Natural	Natural	Natural	68	411	99

Table 1 Attribute table and conversion from Soil Use to Curve Number for the identification if the Soil hydraulic properties.

Simplified conversion Table	*Land Cover Type*	*Description*	*CN*
1	Continuous urban fabric	Dendely popolate areas and services	95
2	Discontinuous urban fabric	Residential areas and green spots	80-85
3	Urban Green areas	Urban parks and sport fields	70
4	Meadows and cultivations	From cultivations to meadows	60-70
5	Forests	From forest to shrubs	50-65
6	Bare soil	Beaches; non vegeated areas	40;75
7	Water bodies	Rivers, lakes, channels, esturies, sea	99

Table 2 Simplified conversion table from Soil Use to Curve Number for the identification if the Soil hydraulic properties.

The SCS-CN method was developed in an empirical framework as such it would need calibration. The impressive sample size used in the calibration in USA watersheds gives reliability and, as proved by different authors (Singh et al., 2002), good method application when used to evaluate the cumulative runoff on durations comparable to the ones used for its calibration, (i.e., 24 h, in most cases the curve number was developed using daily rainfall-runoff records corresponding to the maximal annual flow derived from gauged watersheds (United States Department of Agriculture, 1954; Mishra and Singh, 2003).
More recent applications have also shown the possibility of using the SCS-CN method in a distributed way and on time scales finer than the event scale, so that each cell of a distributed model is described by a CN value and the runoff/infiltration separation is performed at cell scale over a time step (Grove et al., 1998; Moglen, 2000; Gabellani et al., 2008). This is not surprising, due to the general scalability of the continuity equation which is at the base of the method, although a careful recalibration would be needed (Grove et al., 1998; Michel et al., 2005). However, as already pointed out, the nature of the present model allows us to relax the demand for a strict calibration procedure. It is important, in fact, to properly assign the relative importance of the competing processes (i.e. flow concentration vs. flow drainage capacity).

After the CN map compilation it is possible to run the model on the precipitation ensembles for different return periods. The result in terms of maximum water depths in metres is shown in Figure 7. This is the final result of the procedure that can be however post processed in order to obtain a field of maximum water depths on one side and on the standard deviation of such field on the other side. This is done for each return period. An example of such fields is reported in Figure 8 for the Island of Grenada for the catastrophic a return period of 1000 years.

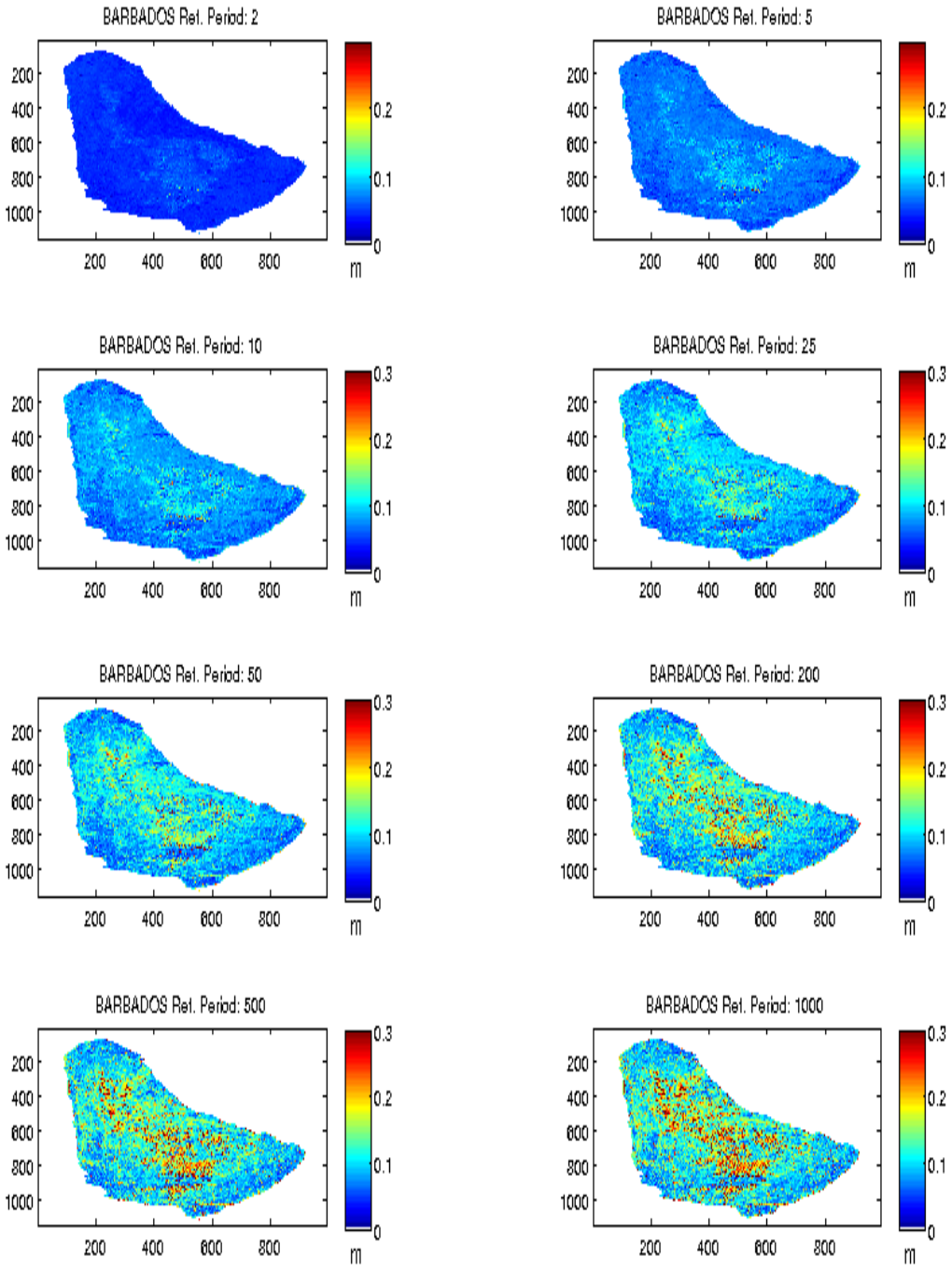

Figure 7 Results in terms of max water depth for different return periods the color ramp is reporting the maximum water depth in meters.

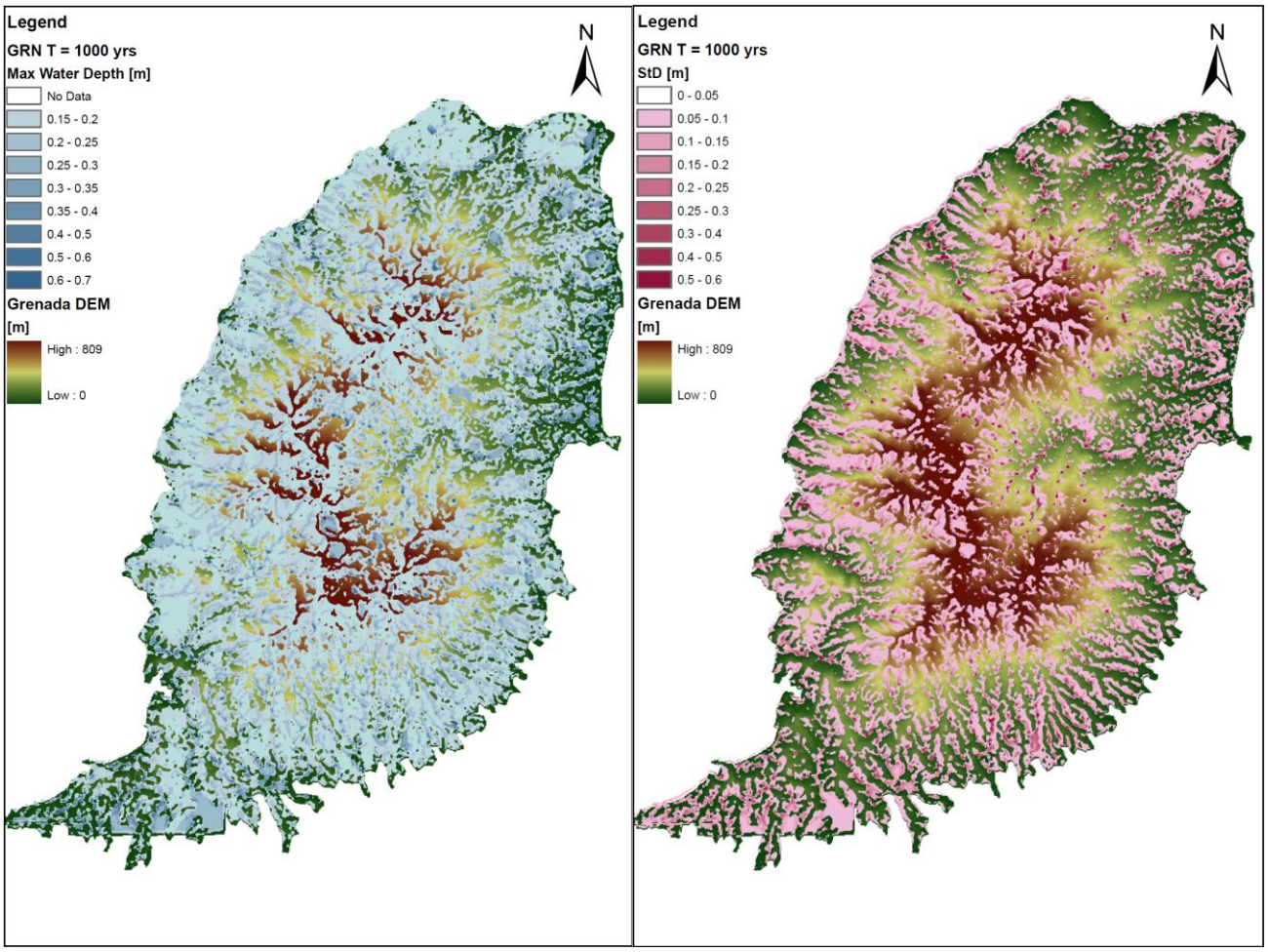

Figure 8 maximum water depths and standard deviation of maximum water depths for the catastrophic event of 1000 year return period layered on the DTM representation of the Island of Grenada

The following figures show the results on Virgin Island layered on Google Earth background. Form the 3D view it is evident the high control exerted by the morphology and by the land use in determining the final result.

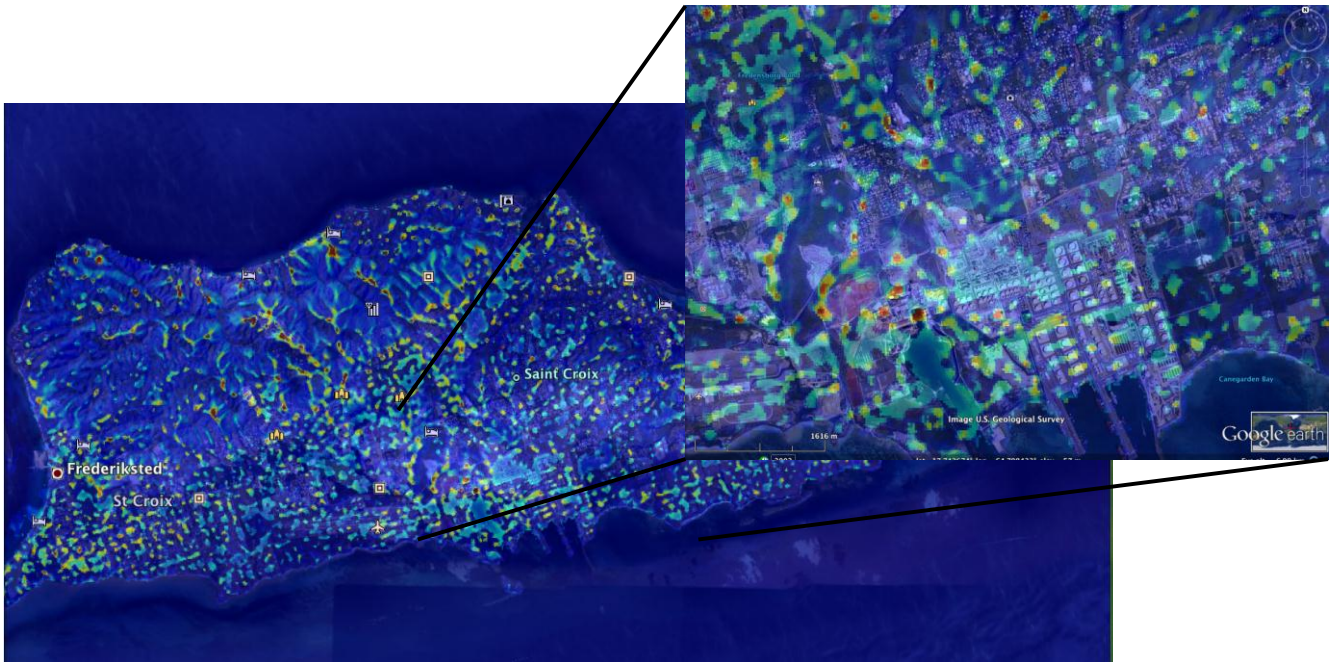

Figure 9 maximum water depths for the 200 year return period layered on the Google Earth, representation of Virgin Island, zoom on the Urban settlement.

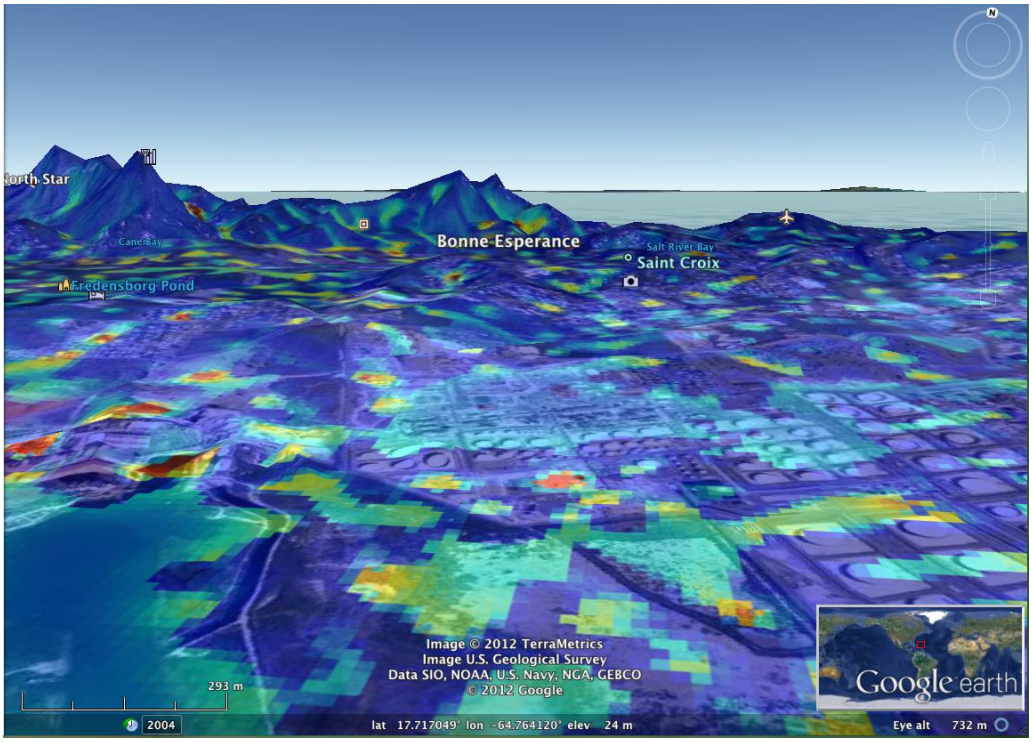

Figure 10 3D view of maximum water depth map for the 200 year return period layered on the Google Earth, representation of Virgin Island, zoom on the Urban settlement.

1.4 Concluding remarks

The model proved suitable for identification of localized flooding hazard in a probabilistic framework as required. The limited information available forced the introduction and shortcuts that should be better verified once additional data are available. As in many cases with regards to localized flooding

the limited amount of calibration information prevented the authors from developing a proper cal/val experiment. However thanks to the model structure the results should be robust enough to drive some indication about the risk that derives form localized flooding in the study areas.

1.5 Bibliography

Per Bak (1996). How Nature Works: The Science of Self-Organized Criticality. New York: Copernicus. ISBN 0-387-94791-4.

Gabellani, S., Silvestro, F., Rudari, R., and Boni, G.: General calibration methodology for a combined Horton-SCS infiltration scheme in flash flood modeling, Nat. Hazards Earth Syst. Sci., 8, 1317-1327, 2008.

Grove, M., Harborand, J., and Engel, B.: Composite vs distributed curve numbers: Effects on estimates of storm runoff depths, J. Am. Water Resour. Assoc., 5(34), 1015–1033, 1998.

Helmer, E.H.; Kennaway, T.A.; Pedreros, D.H.; Clark, M.L.; Marcano-Vega, H.; Tieszen, L.L.; Schill, S.R.; Carrington, C.M.S 2008 Land cover and forest formation distributions for St. Kitts, Nevis, St. Eustatius, Grenada and Barbados from decision tree classification of cloud-cleared satellite imagery. Caribbean Journal of Science. 44(2):175-198

Helmer, Eileen H.; Ruzycki, Thomas S.; Benner, Jay; Voggesser,Shannon M.; Scobie, Barbara P.; Park, Courtenay; Fanning, David W.; Ramnarine, Seepersad 2012 Detailed maps of tropical forest types are within reach: forest tree communities for Trinidad and Tobago mapped with multiseason Landsat and multiseason fine-resolution imagery. Forest Ecology and Management 279:147-166.

Kennaway, Todd; Helmer, E. H 2007 The Forest Types and Ages Cleared for Land Development in Puerto Rico. GIScience & Remote Sensing 44(4):356-382.

Kennaway, Todd; Helmer, Eileen; Lefsky, Michael; Brandeis, Thomas; Sherrill, Kirk 2009 Mapping land cover and estimating forest structure using satellite imagery and coarse resolution lidar in the Virgin Islands. Journal of Applied Remote Sensing 2:023551, pp. 1-27.

Mishra, S. and Singh, V.: Soil Conservation Service Curve Number (SCS-CN) Methodology, Kluwer Academic Publisher, 2003

Moglen, G.: Effect of orientation of spatially distributed curve numbers in runoff calculations, J. Am. Water Resour. Ass., 6(36), 1391–1400, 2000.

Rebora, N., L. Ferraris, J. Hardenberg and A. Provenzale (2006). The RainFARM: Rainfall Downscaling by a Filtered AutoRegressive Model, Journal of Hydrometeorology, ISSN: 1525-755X. Vol. 7 (4), pp. 724-738, DOI: 10.1175/JHM517.1

Singh, P., Frevert, D. K., and Meyer, S.: Mathematical Models of Small Watershed Hydrology and Applications, Water Resources Publications, Highlands Ranch, CO., 2002.

Soil Conservation Service, United States Department of Agriculture. National Engeneering Handbook, Section 4, US Department of Agriculture, Washington, DC, 1954.